CONCENTRATION POLARIZATION OVER REVERSE OSMOSIS MEMBRANES WITH ENGINEERED SURFACE FEATURES

Zuo Zhou, Department of Environmental Engineering and Earth Sciences, Clemson University, 342 Computer Ct, Anderson, SC 29630
zuoz@g.clemson.edu, Ph: 352-283-0433
David A. Ladner, Clemson University, Anderson, SC
Steven T. Weinman, University of Alabama, Tuscaloosa, AL
Sapna Sarupria, Clemson University, Clemson, SC
Scott M. Husson, Clemson University, Clemson, SC
Ilenia Battiato, Stanford University, Stanford, CA

Introduction

Concentration polarization (CP) is difficult to measure experimentally, so building models can be a better way to characterize and quantify it. Many studies have focused on building analytical models to predict CP, in which the classic film theory provides an estimate of the degree of CP based on the flux and mass on both sides of the membrane system (Zydney 1997). Numerical models, specifically with computational fluid dynamics (CFD), have been developed to combine Navier-stokes, continuity, and convective-diffusion equations to solve for the CP layer and water permeation flux condition (Kim and Hoek 2005; Lyster and Cohen 2007).

A critical piece to the numerical modeling accuracy is to use fully coupled flow and transport equations. In one class of the modeling, people have used analytical models to theoretically predict permeation flux, and use numerical simulation to predict flow and mass transfer (Ishigami and Matsuyama 2015). Peng et al (Xie, Murdoch, and Ladner 2014) studied fouling in spacer filled channels with equations fully coupling flow and transport, and predicted fouling mitigation that matched the lab results decently. In our models, our flow and transport equations are combined to solve for mass transfer equations. Osmotic pressure is linearly related to salt concentration, and flux is calculated through the pressure difference. By incorporating diffusivity through the convective diffusion equation, we are able to predict permeate flux decline more accurately.

The main goal of this study is to investigate hydrodynamic influence on patterns ranging from 2 μm up to 512 μm. And for each size, we built ten geometry shapes that cover elementary shapes including line and grooves, pillars, chords, pyramids, and bio-inspired patterns. This paper gives a detailed overview on important characteristics including CP, shear stress, pressure drop, velocity distribution, permeate flux and so on. In the end, we built analytical models to compare with the numerical results, and analyzed how patterns affected the mass transfer coefficient.

Materials and Methods

Geometries studied

Multiple models of RO membrane systems with varied geometries were built for analysis. The geometries include flat, several line and groove patterns, rectangular and circular pillars, circular chords and pyramids, which are based on the same size range. In addition to these elementary patterns, a few bio-inspired patterns including shark skin and lotus leaves were also created for simulations. Models were partly created with SolidWorks, solved with Comsol Multiphysics 5.3 and run on the Palmetto Cluster, Clemson University's primary high-performance computing (HPC) resource.

For the boundary conditions, we have run models at different salt concentrations and with different diffusion coefficients, but the conclusions of this study (e.g. the comparative CP results among patterns) did not change, so here we are only reporting one salt concentration and velocity. To be consistent with an ongoing project in our lab, we used inlet velocity (u_{in}) as 0.1 m/s, feed (inlet) concentration as 0.025 M $MgSO_4$, which is calculated from 3000 ppm $MgSO_4$. The diffusion coefficient is 10^{-9} m^2/s.

At the outlet, the pressure was set to be 2758 kPa (400 psi). Viscous stress and diffusive flux at the outlet were assumed to be negligible. The boundary on the top was set as a wall moving at a velocity equal to u_{in}, parallel to the membrane. The flux velocity normal to the wall at the membrane u_m is set as

$$u_m = A(\Delta P - a_{osm} c_w) \qquad (1)$$

Where A is the water permeability of membrane that is equal to 5.24×10^{-12} m/(s·Pa), a_{osm} (osmotic coefficient) is 4872 Pa/(mol/m^3).

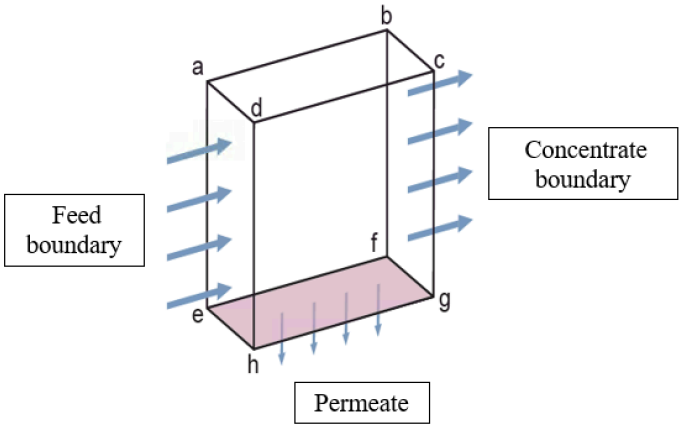

Figure 1. Conceptual model for the membrane simulations. The block represents the water- and solute-filled space above the RO membrane. At wall abcd water is moving with a velocity adjusted based on the Hagen Poiseuille equation, and at the feed boundary, the inlet velocity is set according to the model size, both assuming the full channel is 16 mm high. Inlet concentration is 0.025 M. Concentrate boundary is 2800 kPa. Wall abfe and dcgh are periodic boundaries. The membrane is at the bottom (pink color).

In these models, a block was used to represent the membrane system. Data including pattern lengths, heights, distances and the fillets that were used to curve the edges are shown in the table below. Pattern sizes range from 2 μm to 512 μm, with each time the length increasing four times. The distance between patterns is the same as the length, while the height of the pattern is equal to half of the length (see Table 1. For details). Edges were curved by adding fillets with a radius that is one fifth of the height.

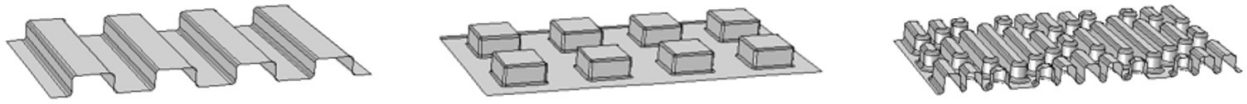

Figure 2. Examples of elementary geometries and bio-inspired patterns. Left: line and groove rectangular patterns. Middle: rectangular pillars. Right: shark skin.

Table 1 Parameters of the geometries

Feature Length (μm)	Feature Height (=0.5·Length) (μm)	Between-Feature Distance (=Length) (μm)	Fillet (=0.2·Height) (μm)
2 μm	1 μm	2 μm	0.2 μm
8 μm	4 μm	8 μm	0.8 μm
32 μm	16 μm	32 μm	3.2 μm
128 μm	64 μm	128 μm	12.8 μm
512 μm	256 μm	512 μm	51.2 μm

In these models, all the geometries are proportional to the pattern sizes.

Governing equations

Fluid and transport of magnesium sulfate (the assumed rejection rate is 100%) inside the membrane system was described by Eqs. (2)-(4).

$$\rho\left(\nabla\cdot\mathbf{u}\right)\mathbf{u} = -\nabla P + \frac{\mu}{2}\nabla\cdot\left(\nabla\mathbf{u} + \nabla\mathbf{u}^{T}\right) \tag{2}$$

$$\nabla\cdot\mathbf{u} = 0 \tag{3}$$

$$\nabla\cdot c = D\nabla^{2}c \tag{4}$$

Where $\boldsymbol{u}$ is the fluid velocity vector, t is time, ρ is density, P is pressure, μ is dynamic viscosity, c is concentration, and D is the diffusion coefficient. Navier-Stokes equations include conservation of momentum (Eq. (2)) and conservation of mass (equation (3)). Equation (4) is the convection-diffusion equation. Due to the full coupling of momentum and mass transport, the solutions are simultaneous, combining Navier-stokes, continuity and convective diffusion equations to show the most accurate results.

Results and Discussions

Concentration and Shear Stress

In nanometer and micrometer scale, the concentration profiles for most models showed a low concentration at the entrance with a gradual increase towards the downstream end. Concentration polarization was manifest with a high concentration near the membrane surface and a decrease towards the bulk solution. For patterned membranes, the concentration accumulation is more intense before getting to the valley, but less intense after coming out of the valley. An example of concentration profiles of membranes with line and groove rectangular patterns is shown in Figure 3 (left).

Shear stress in these models was highest in the apex of the patterns and lowest in the valleys. The value reduced as it entered further into the channel with each peak value being smaller. The low shear stress corresponds to high concentration area.

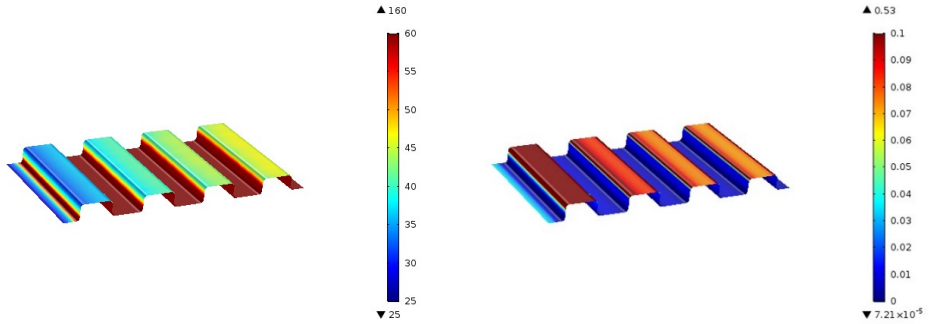

Figure 3. Concentration distribution (left) and shear stress (right) along the membrane surface for line and groove rectangular 512 μm patterns.

Concentration Polarization (CP) Factor

The method to compare CP is by calculating CP factor, defined as the ratio of salt concentration at the membrane surface to bulk concentration (c_w/c_f). In this paper, CP factor is calculated as the ratio of salt concentration at the patterned membrane surface to inlet concentration (25 mol/m^3). Several models were run and results were collected.

Results indicate that none of the patterns, and none of the pattern sizes, decrease concentration polarization. Compared to a flat membrane, they all resulted in higher CP factors.

Velocity Distribution and Streamlines

In these models, we adjust the velocity based on a total channel height of 16 mm. To do so, we applied a moving wall on the other side of the channel and applied a velocity calculated through the Hagen Poiseuille equation.

$$u = \frac{3}{2}u_m[1 - \left(\frac{y}{H}\right)^2] \quad (5)$$

Smaller patterns resulted in the distortion of velocity distribution, but they did not cause any significant interruptions. The velocity at the valley around the corner is the lowest, indicating a potentially high salt concentration accumulation.

Analytical Results vs. Numerical Simulations

In the analytical results, we built up the correlation between Reynolds number, Schmitt number, and Sherwood number.

$$Sh = 1.85\left(Re \cdot Sc \cdot \frac{d_h}{L}\right)^{0.27} \quad (6)$$

Sherwood number is the rate of convective mass transfer to rate of diffusive mass transport.

$$k = Sh \cdot \frac{D}{d_h} \quad (7)$$

$$\frac{c_m}{c_b} = exp\left(\frac{J}{k}\right) \quad (8)$$

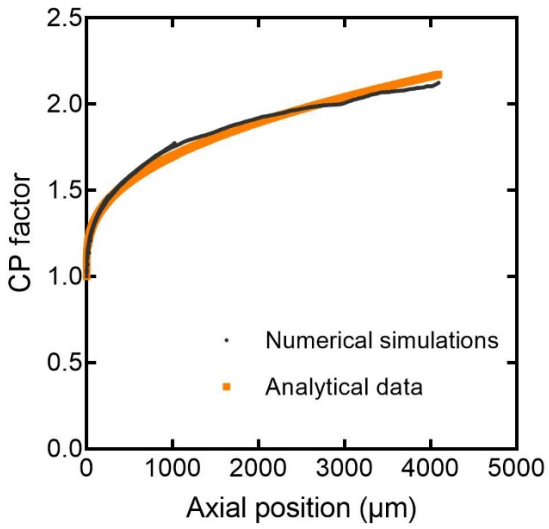

Figure 4. Analytical results in comparison to numerical simulations for 5 flat models.

Numerical simulations fit the analytical results very well, reassuring us of the accuracy of these models.

Conclusions

Patterned membranes with various sizes and shapes were studied and analyzed. Velocity distribution, concentration, shear stress, permeate flux and pressure gradient were plotted and compared. None of the patterns decreased CP, despite the fact that some vortices were developed near the membrane surface. Our study confirmed the influence of flow characteristics and shear

stress to changing concentration distribution in a membrane system. Higher shear stress at the apex resulted in lower concentration, whereas lower shear stress at the valley caused more CP, resulting in a higher CP value on average. Our models provide a systematic examination over a wide pattern size range, and they covered most of the common sizes of patterns that can be fabricated. Our models showed that reduced foulants on patterned membranes observed in the lab or simulated in other models might not be due to the mitigation of CP. Other factors such as system hydrodynamics or operating conditions can cause different fouling results.

Acknowledgements

This work is funded by the National Science Foundation under CBET grant #1534304. Clemson University is acknowledged for generous allotment of compute time on the Palmetto cluster.

References

Ishigami, Toru, and Hideto Matsuyama. 2015. "Numerical Modeling of Concentration Polarization in Spacer-Filled Channel with Permeation across Reverse Osmosis Membrane." https://doi.org/10.1021/ie5039665.

Kim, Suhan, and Eric M V Hoek. 2005. "Modeling Concentration Polarization in Reverse Osmosis Processes." *Desalination* 186 (1–3): 111–28. https://doi.org/10.1016/j.desal.2005.05.017.

Lyster, Eric, and Yoram Cohen. 2007. "Numerical Study of Concentration Polarization in a Rectangular Reverse Osmosis Membrane Channel: Permeate Flux Variation and Hydrodynamic End Effects." *Journal of Membrane Science* 303 (1–2): 140–53. https://doi.org/10.1016/j.memsci.2007.07.003.

Xie, Peng, Lawrence C. Murdoch, and David A. Ladner. 2014. "Hydrodynamics of Sinusoidal Spacers for Improved Reverse Osmosis Performance." *Journal of Membrane Science* 453 (March): 92–99. https://doi.org/10.1016/J.MEMSCI.2013.10.068.

Zydney, Andrew L. 1997. "Stagnant Film Model for Concentration Polarization in Membrane Systems." *Journal of Membrane Science* 130 (1–2): 275–81. https://doi.org/10.1016/S0376-7388(97)00006-9.